ACS OMEGA

Open Access

http://pubs.acs.org/journal/acsodf

Mini-Review

Simplified Biochemical Analysis Using p-Block Metals and Their Compounds with Silver—Surface Enhancement from the Point of View of Electronic Structure

Rosen Todorov* and Temenuga Hristova-Vasileva

Cite This: *ACS Omega* 2025, 10, 19243−19255

Read Online

ACCESS | Metrics & More | Article Recommendations | Supporting Information

ABSTRACT: This mini-review presents recent trends in the field of surface-enhanced spectroscopies, which are increasingly gaining ground for biomolecule detection. The paper discusses the role of electromagnetic and chemical bonding mechanisms for an explanation of Raman scattering and fluorescence enhancement. The charge transfer (CT) effect, which is involved in the chemical mechanism, plays an important role in changing the polarizability and is decisive in enhancing certain Raman scattering bands and fluorescence emission. The CT effect is determined by the band structure and the energy of the excitation radiation by which photoelectrons and holes with different energies are generated. Here we analyze the changes in the band structure of silver by adding p-block metals as well as the possibility to control CT and to enhance specific Raman bands through their engineering.

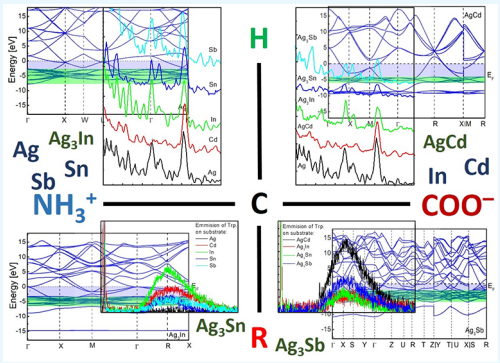

1. INTRODUCTION

Human beings are 60% water. This is a statement that every one of us has heard. Water keeps us in shape, both literally and figuratively speaking. It supports the functioning of all other 40% of the human molecular structure, including proteins, fats, carbohydrates, hydroxyapatite, and nucleic acids.[1]

Apart from our personal molecules, our bodies interact, internally and externally, with other organisms, such as bacteria, fungi, and viruses, by creating a healthy symbiosis, called human microbiome, that ensures our well-being.[1]

The microbes are independent living organisms that can be seen through a microscope. They all possess their own nucleic acid fragments (DNA or RNA).[1] When the population levels of microbes in the human body are increased, they are often referred to as pathogens, causing discomfort and diseases.

Bacterial cells and virus particles generally consist of nucleic acids, lipids, and proteins, as the part of proteins is above 50% of the whole composition. On the other hand, almost every cell in our bodies possesses proteins, and they play a major role in the biochemical processes for prevention of infection and fighting infections.[1]

Since the proteins are formed by transcription of DNA to RNA, and its translation through ribosomes and binding of amino acids in a desired sequence,[1] it can be said that the fight in our bodies is between the genetic codes of the pathogens and of our human cells, and the main fighters are their amino acids.

Hundreds of amino acids exist in nature, but 22 are the most important of them, which are involved in protein production. They are known as α-amino acids. All of them are basically made of carbon, oxygen, and nitrogen and commonly consist of four main parts: amino group, carboxyl group, hydrogen atom, and R-group, also called side chain, that carry the main data of the specific amino acid.

The change of the pH influences the properties of the amino acids by mainly causing ionization of their amino and carboxyl groups,[2] as well as their overall solubility ability.[3]

The amino acids, as well as their corresponding peptides and proteins, tend to form coordination complexes with heavy and transitional metals.[4] In general, in basic medium the amino acids bond mainly through their carboxylate group, and in acidic medium, through their amino group, while the processes in the more complicated cases, such as peptides and proteins, evolve intrinsic chemical reactions, a variety of cases and binding mostly through the side chains, due to the already occupied amino and carboxylate groups.[5]

This ability of the amino acids to bind metallic ions is essential for living organisms.[6] On one hand, it can neutralize and thus reduce the concentration of unwanted electrolytes through chelation, and on the other, by the same way it can reduce the effective concentration of undesired microbes.[6a,b]

When we are ill, regardless of whether it is due to an external factor, such as a microbe, for example, or an internal dysfunction,

Received: February 15, 2025
Revised: April 7, 2025
Accepted: April 28, 2025
Published: May 7, 2025

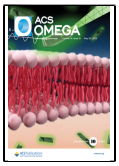

before any treatment one has to find out what causes this discomfort. Therefore, there are methods for determination and evaluation of the types and levels of biochemical objects and micro-organisms in our bodies. Since all living organisms possess amino acids, their interaction with transitional and heavy metals gives an essential advantage in diagnostics as well, due to the signal enhancing properties of the metallic particles.[7]

In the next section, we will present a brief overview of the modern Surface enhanced spectroscopies, playing an increasingly important role in the field of molecular diagnostics, as well as the main principles and mechanisms influencing the Raman scattering and Fluorescent emission surface enhancement and their importance in achieving enhancement of specific markers in the spectra in order to develop various diagnostic methods.

We focused on the role of the electronic structure of the substrate in energy transfer, which determines the enhancement of different bands in surface-enhanced Raman scattering (SERS) and surface-enhanced fluorescence (SEF) spectra. With this aim, we review the changes in the electronic structure of intermetallic compounds and present an analysis of the influence of substrates made of silver and p-block elements (Cd, In, Sn, and Sb) on the SERS and fluorescence spectra of L-tryptophan.

2. SURFACE ENHANCED SPECTROSCOPIES IN BIOMOLECULE DETECTION

Biomolecule detection for analytical, medical, biochemical, and pharmaceutical purposes requires rapid identification of various chemical compounds and the chemical reactions in which they participate. This is why the methods allowing direct identification of chemical compounds and processes occurring in living organisms, such as Raman spectroscopy, Fourier transform infrared (FTIR) spectroscopy, and fluorescence spectroscopy, have found wide application.[8] The effect of Raman enhancement of pyridine adsorbed on metal electrodes, first observed more than 50 years ago, makes it possible to significantly increase the sensitivity of these spectroscopic techniques and to develop a new field, laying the foundation for the so-called enhanced spectroscopies, which nowadays include surface-enhanced Raman scattering (SERS), surface-enhanced fluorescence (SEF), surface-enhanced infrared absorption (SEIRA), surface-enhanced hyper Raman scattering (SEHRS)- and surface-enhanced Ramanoptical activity (SEROA).[9]

The increased sensitivity in comparison to the classical methods and the ability of these techniques, under special conditions, to register and analyze single molecules, have made them indispensable, especially in the field of Molecular diagnostics, for analysis of biological markers in the genome and proteome during identification of diseases at the molecular level.[10] A review of the application of SERS in modern techniques for Molecular diagnostics such as Specific High-Sensitivity Enzymatic Reporter UnLOCKing (SHERLOCK) and DNA Endonuclease-Targeted CRISPR Trans Reporter (DETECTR), as well as the perspective of SERS in gene-editing tool SERS-based CRISPR/Cas (SERS-CRISPR) was made by the authors of ref 10a.

A number of publications report an existing correlation between the reduction in the concentration of specific amino acids, in particular tryptophan and tyrosine, glycine, phenylalanine, histidine and a combination of proline, glycine and hydroxyproline (collagen),[11] which makes them potential biomarkers and allows the development of procedures for the detection and diagnosis of some disease at earlier stages. L-Tyrosine and L-tryptophan play an important role in a number of biochemical processes related to mental disorders, such as depression, neurotransmitters in the case of neurological diseases (epilepsy), or neurodegenerative disease (Alzheimer's and Parkinson's diseases), proteins for diagnostics of cancer, DNA analysis.[8a]

Furthermore, the positions and intensities of the Raman peaks of these amino acids strongly depend on the nature of the environment in proteins. Based on this behavior, various procedures using SERS have been developed that track the intensity of certain Raman bands to pinpoint the potential emergence of a specific disease or provide evidence of infection,[11d] biomarkers for cancer detection,[11d,11] and virus detection.[11e]

The absorption bands of biological substances, such as nucleic acids and amino acids, are found in the UV region.[12] Fluorescence spectroscopy is also an important method in the study of biological objects. Although it does not provide direct information about the chemical composition, the fluorescent emission of tryptophan and tyrosine excited by UV radiation is highly sensitive to microenvironment variations, a problem that has been intensively studied since the 1960s.[12a] Their emission strongly depends on local structure and dynamics.[12d]

3. BASE FACTORS FOR SIGNAL ENHANCEMENT

3.1. Localized Surface Plasmons and Hot-Spots in Surface Enhanced Raman Spectroscopy (SERS). The molecular vibrations observed only in Raman spectra are related to the change in the polarizability of the analyzed molecule. In the case of SERS, two major types of interaction of the molecule with the nanostructure can change its polarizability and cause enhancement of the Raman signal: electromagnetic enhancement, in which large local fields are created by electromagnetic resonances occurring near the metal surface, and chemical or charge-transfer effect, in which the molecular polarizability is affected by the interaction between the studied molecule and the metal surface.[13]

Two factors are of great importance in order to boost the signal and to achieve reproducibility in SERS: the instrument conditions and the substrate.[13a] The laser beam drives the localized surface plasmons into resonance or excites the localized surface plasmon resonance (LSPR). An important condition for achieving an effective electromagnetic amplification in SERS is tuning the frequencies of the LSPR and laser radiation. Thus, amplification occurs in both the laser excitation radiation and scattered radiation of the nanostructures.

The complex permittivity, ε, determines the plasmonic response of metal nanostructures and the reaction of a substance when it interacts with an external electromagnetic field,[14] and is a function of the electronic structure and the transitions in the material. In the case of metals, ε can be considered as the sum of the contributions of free electrons and the contribution from interband transitions.[14a−c] Of essential importance for the efficiency of LSPR excitation is the real part of the complex permittivity to be negative, while the optical loss related to its imaginary part is minimal. This rule determines that different materials and structures can be effective in a certain spectral region. Work is being done in two directions for this: one is to find plasmonic materials with optimal complex permittivity from the point of view of realizing LSPR, and the other is to model nanostructures to obtain maximum localization of electrons.

It is well-known that the noble metals gold and silver are most effective for LSPR excitation in the visible spectral region. The use of alloys of noble metals (Ag, Au and Cu)[14b] allows further

https://doi.org/10.1021/acsomega.5c01439
ACS Omega 2025, 10, 19243−19255

tuning of the LSPR excitation efficiency, while the p-block metals (Al, In)[14d] and their alloys with noble metals allow tuning of the LSPR in the short-wavelength part of the visible region,[14a,e] or in the UV spectral region.[14a,c]

The most widely used nanostructures for SERS are spherical silver and gold colloids.[15] The possibility to design LSPR using different geometric shapes evokes growing interest in lithographic methods and self-organization processes for preparation of nanostructures.[16] Preparation procedures and optical characterization for plasmonic nano- rods,[15] triangles[16a] and iso-Y nanoparticles[16c] have been reported. It should be mentioned that many materials with amplifying properties, based on compounds and composites including oxides, rare earth elements, 2D materials (graphene, graphene oxide, 2D transition metal dichalcogenides, MXene) etc., which give promising results were developed recently.[17]

The distance between the analyzed molecule and the metal nanostructure is of particular interest. Under the influence of an external field, the metal nanoparticles are polarized and can be considered as electric dipoles if they are smaller than 40−60 nm in size, while at larger NP sizes higher multipole moments (quadrupoles and octopoles) start to contribute.[14f] Each particle senses the influence of the induced dipoles of the surrounding particles if they are close enough. When the electric field vector is parallel to the line connecting the centers of two particles, then an extreme field enhancement can occur in a small spatial region between NPs.[15,18]

A number of works, devoted to modeling of the electric field between two charged spheres and their dipole polarizability, show that the maximal enhancement of electric filed is obtained when the distance between the particles is less than 10 nm,[14d] and this effect decreases sharply at larger distances.

The molecule distance, orientation, and affinity toward the metal surface also determine the SERS signal. Surface selection rules are reported, according to which the most intense bands in SERS spectra are those given by vibrations inducing polarization of the adsorbate electron cloud perpendicularly to the metal surface.[12b]

Although the electromagnetic theory provides a reasonable explanation for the origin of the enhancement in Raman scattering, it fails to clarify the variety of magnitudes of the enhancements among different vibrational modes. Thus, a chemical mechanism explaining the Raman scattering enhancement has been proposed, where the charge transfer between the substrate and molecules is believed to alter the electron density distribution of molecules, resulting in greater polarizability.[15,18] This mechanism strongly influences the fluorescence emission, and we will discuss it in the following sections.

3.2. Fluorescence Quenching in Surface-Enhanced Fluorescence (SEF). As in SERS, in SEF the way the molecule is attached to the metal particle is also of great importance for energy transfer. Fluorescence emission occurs when the photoexcited electrons radiatively relax to the ground states. However, there are a number of processes in which electrons in these excited states can relax nonradiatively. These are collectively known as "fluorescence quenching". Fluorescence quenching is due to processes like electron transfer, energy transfer and complex formation:[19]

- In the case of metal nanoparticles, significant fluorescence quenching occurs when the emission spectrum overlaps with the plasmon absorption band of the nanostructures. Then an excited electron from the organic molecule (donor) can pass into the conduction band of the metal (acceptor) and relax to the Fermi level of the metal nanoparticle (Figure 1a).

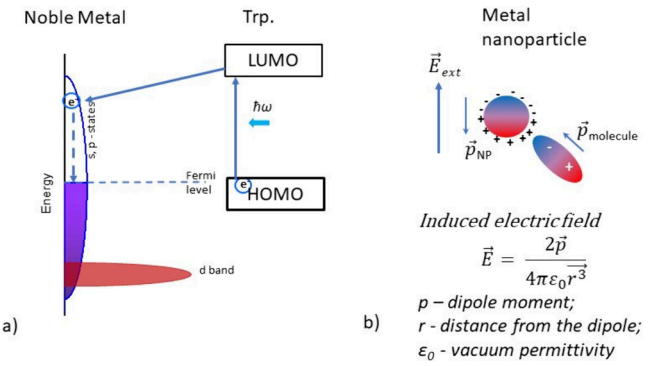

Figure 1. Possible electronic processes leading to fluorescence quenching. Relaxation of an excited electron from the LUMO orbitals to the Fermi level (a) and influence of the orientation of the dipole moments $\vec{p}_{NP}$ and $\vec{p}_{molecules}$ of metal nanoparticle and molecule, respectively, in case of direct interaction of an organic molecule and a metal nanoparticle (b).

- The polarization of the external electromagnetic field and the orientation of the molecule also have an impact on the fluorescence quenching effect. Since the electric field of metal nanoparticles and organic molecules has a dipole character, the destructive combining of the dipole moment of the molecule and the induced dipole moment of the metal nanoparticle causes reduction of the fluorescence signal (Figure 1b).
- The formation of a chemical bond can significantly change the donor's and acceptor's electronic structure and, respectively, the absorption and emission bands. Strong coupling prevails over the energy engaged in the heating process unless the molecule is extremely close to the metal surface. Therefore, in most cases of SEF analyses, for achievement of signal amplification, a dielectric separation layer (spacer) is used to provide a distance between the fluorophore and the metal nanoparticle.[11b]

Research studies[19b,c] on the distance between the fluorophore and the nanostructure show that the emission intensity undergoes a quenching effect only when the distance between the nanoparticles of the dimer is very small, which means that the strong coupling prevails over the heating energy. Furthermore, the surrounding environment can affect fluorescence quenching because of the presence of various factors including volatile organic compounds (VOCs). This is why the phenomenon finds application in the design of sensors that are sensitive to small changes in the environment and possess sensitivity in the range of nanomoles per liter (nM/L).[20]

Considering the distance between the light-sensitive molecules (chromophores) and metal-nanostructures, two mechanisms for energy transfer may be important: Förster resonance energy transfer (FRET) and nanometal surface energy transfer (NSET).

FRET takes place when the metal particle and organic molecule are located close to each other at distances less than 10−20 nm. A donor chromophore, initially in its electronically excited state, may transfer energy to an acceptor chromophore through nonradiative dipole−dipole coupling.

https://doi.org/10.1021/acsomega.5c01439
ACS Omega 2025, 10, 19243−19255

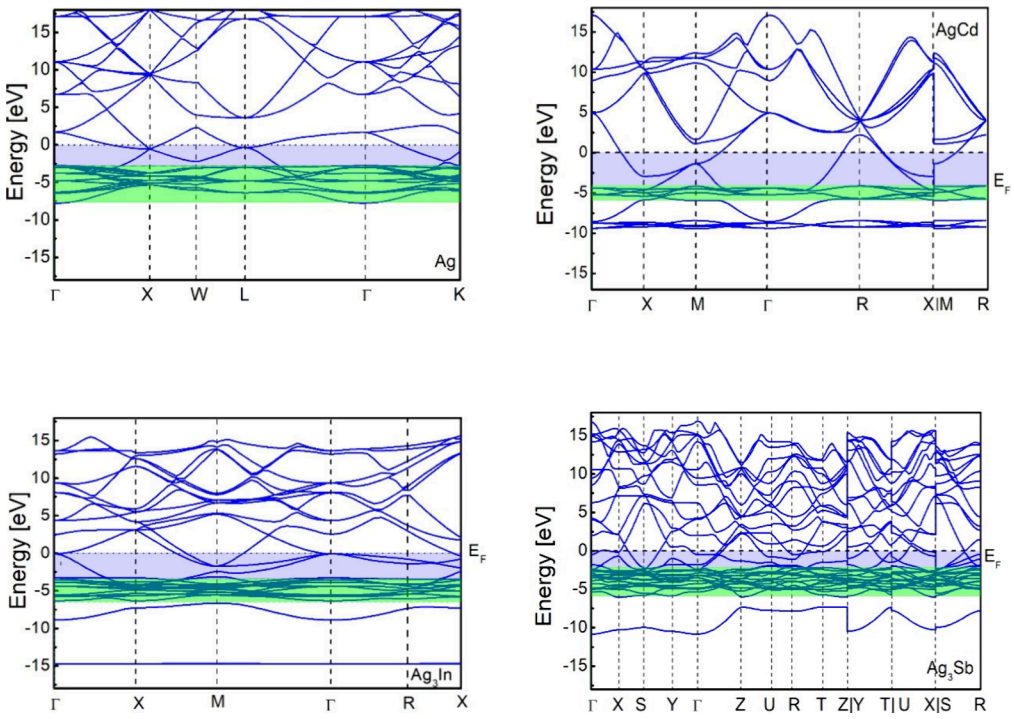

Figure 2. Band structure in the $E(\vec{k})$ space of intermetallic compounds of silver and p-block metals. The 4d electronic state of silver is marked in green, and the energy gap separating it from the Fermi level is indicated in light purple. Fermi energy, E_F, is set to 0.

The energy transfer between the nanostructure and the molecule at larger distances, in the range of 40 to 100 nm, have been investigated in.[19c] The authors concluded that in this case NSET is observed, which is a nonradiative dipole-surface dipole energy transfer process occurring from an excited state of a donor fluorophore to a proximal surface of an acceptor nanoparticle surface.

In the next section, we will discuss how the chemical composition and electronic structure of the nanostructure material play a significant role in both electromagnetic amplification and charge transfer.

4. ELECTRONIC STRUCTURE OF PLASMONIC MATERIALS AND CHARGE TRANSFER

As previously mentioned, the main and most widely used and studied enhancing materials are the noble metals and the alloys formed between them.[14b,21] The conduction band of the metals (Cu, Ag, Au) from group 11 of the Periodic table of elements consists of hybridized *s* and *p* electronic states and a *d* band with a significantly higher density of states, and *d*-to-*sp* interband electronic transitions occur at ∼2.1 eV (∼590 nm) for Cu, ∼2.4 eV (∼516 nm) for Au and ∼3.8 eV (∼ 320 nm) for Ag.[14b]

It can be expected that the electron transfer and formation of chemical interactions in the cases of SERS and SEF are determined by the energy spectrum of free electrons and holes generated through interband transitions. The application of different current carriers generated as a result of intraband and interband transitions in nanostructures of gold and Au−Cu alloys in the field of photocatalysis has recently been discussed in a number of works.[22] According to the authors of 22a when light whose photons have an energy lower than that required for interband transitions interacts with free *s* electrons in metal nanostructures hot photoelectrons occupying energy states above the Fermi level are generated. The interband transitions result in highly energetic holes in the *d* band far below the Fermi level and excited electrons in the *sp* band near the Fermi level. The formed hole of high energy can interact with oxidants. Research investigations[14b] of the variation of the plasmon frequency in Ag−Au, Ag−Cu, Au−Cu alloys demonstrate that the energy of the *d*-to-*sp* transitions can be tuned in ranges limited by the energies for interband transitions of the metals involved in the alloy.

Earlier, we presented an extensive overview of the properties and qualities of metals from the p block of the Periodic table of elements and their alloys with noble metals as plasmonic materials.[14c] The advantage of using the most simplified substrates, as is the case with single- and double-component metallic layers, is their simple and cheap preparation and the possibility of easily tuning the desired operating frequency. The possibility of preparation of 2D structures from p block metals (Bi, Ga, In, Sn and Pb) makes them prospective materials for SERS, sensing, bioimaging and photothermal therapy.[23] The use of intermetallic alloys and compounds of different p-block elements and noble metals (silver or gold) allows further expansion of the interval in which the energy required for *d*-to-*sp* interband transitions can be varied. In this case, due to the larger number of valence electrons on the p-block, the Fermi energy increases, and accordingly, the energy for interband transitions from the *d* level of silver (or gold) increases. It should be kept in mind that the *d* level of p-block metals lies significantly below the Fermi energy and higher photon energies of 10−25 eV are required for intraband transitions.[24]

The contribution to intraband transitions in the spectral interval 1−4 eV can be expected from their *s* and *p* electrons.[24a] The analysis of the valence band by X-ray photoelectron spectroscopy (XPS) and density functional theory (DFT) calculations,[24b,e] as well as the spectrum of complex permittivity determined by spectral ellipsometry,[24f] show a shift of the *d* level further below the Fermi level and an increase in the energy required for interband transitions. The DFT calculations predict

https://doi.org/10.1021/acsomega.5c01439
ACS Omega 2025, 10, 19243−19255

that the most significant changes are observed in alloys of the Ag−Cd and Ag−Sn systems.[24e] In Figure 2 the band structure and the density of states (DOS) from DFT calculations are presented, as well as the electronic density of states in the valence bands of Ag_3In, AgCd and Ag_3Sb, experimentally determined through XPS. A description of the DFT calculations is given in the third point of the Supporting Information (Suppl. 3). It can be seen that the addition of p-block metals leads to an increase in the energy gap between the Fermi level and the 4d electronic state of silver due to an increase in the number of free electrons, which in turn increases the Fermi energy, E_F. The most significant shifts of the 4d level of silver are observed in the case of AgCd and Ag_3Sn, while the smallest changes appear in the case of Ag_3Sb. From the electron density of states (DOS) presented in Figure 3, we can determine the upper limit of the 4d

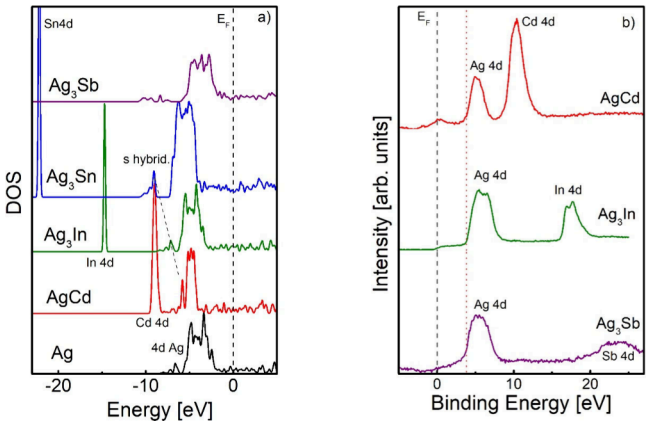

Figure 3. Electronic density of states (DOS) of intermetallic compounds of silver and p-block metals, determined by (a) density functional theory (DFT) calculation and (b) X-ray photoelectron spectroscopy (XPS).

level of silver, i.e., the minimum energy required for transitions to the Fermi level, as follows: 2.15 eV in the case of Ag, 4.15 eV for AgCd, 3.27 eV for Ag_3In, 3.74 eV for Ag_3Sn, and 2.22 eV for Ag_3Sb.

According to published results, the interband transitions in alloys of Ag with p-block metals occur in the range of 2−4 eV,[14a,c,24f,25] while the plasma frequency (the so-called epsilon zero point) is shifted into the UV spectral region in the range of 5 − 8 eV, which allows excitation of LSPR in the ultraviolet spectral region.[25,25c,d]

A schematic diagram of the processes of the excitation of charged carriers, including the formation of hot electrons and holes, is presented in Figure 4a. In the case of tryptophan, the Fermi energy of silver (−5.49 eV[26]) is close to the theoretically determined energy of the HOMO of tryptophan (~4. 77 eV[27]). In Figure 4b, a case of heterotransition and possible electron transitions between the electronic states of silver and tryptophan is considered. The formation of and their interaction with cations and anions in the case of photocatalysis has recently been discussed.[22] According to the authors, hot electrons can transition to the LUMO levels of the amino acid. There are two processes for the formation of hot holes, except through the described process of interband transitions, hot holes can be generated by LSPR. According to[18b] the hot holes can accelerate the oxidation process of metals and in the case of amino acids they support the reaction of the metal nanoparticle with the carboxylate COO^- group.

The use of intermetallic alloys makes it possible to obtain plasmon resonances and interband transitions occurring in well-separated spectral windows, to selectively determine the interaction of molecules, and, accordingly, to control the intraband and interband hot carriers, which can be selectively excited by choosing the appropriate excitation wavelengths.

5. SERS ANALYSIS

In recent years, there has been growing interest in studying the possibility of engineering the electronic structure and providing active sites for molecular adsorption of the materials from which nanostructures are made.[28] Using nanostructures of different metals or alloys for SERS can affect the enhancement of certain bands in the Raman spectra of amino acids. In the case of electron transfer, by using different supports it is possible to observe different enhancement, which complicates the comparison of SERS spectra and can be easily controlled by choosing the wavelength of the exciting laser radiation.[17c] Research in the field of SERS analysis of amino acids is still in its early stages.[28] In the case of tryptophan, data are found where different spherical

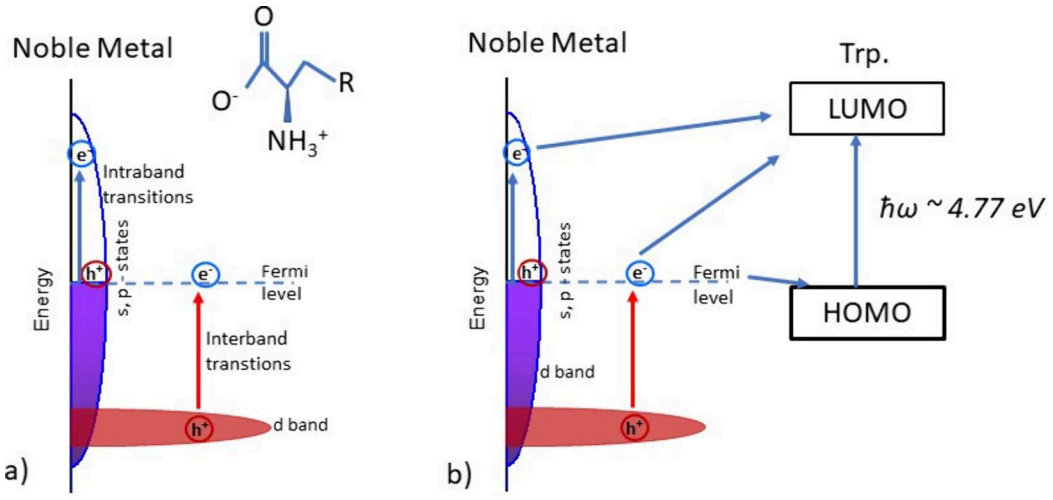

Figure 4. Schematic diagrams of electron states and transitions in a metal particle for reaction with the functional groups of amino acid (a); and electron transitions in the case of a metal-tryptophan complex (b).

https://doi.org/10.1021/acsomega.5c01439
ACS Omega 2025, 10, 19243−19255

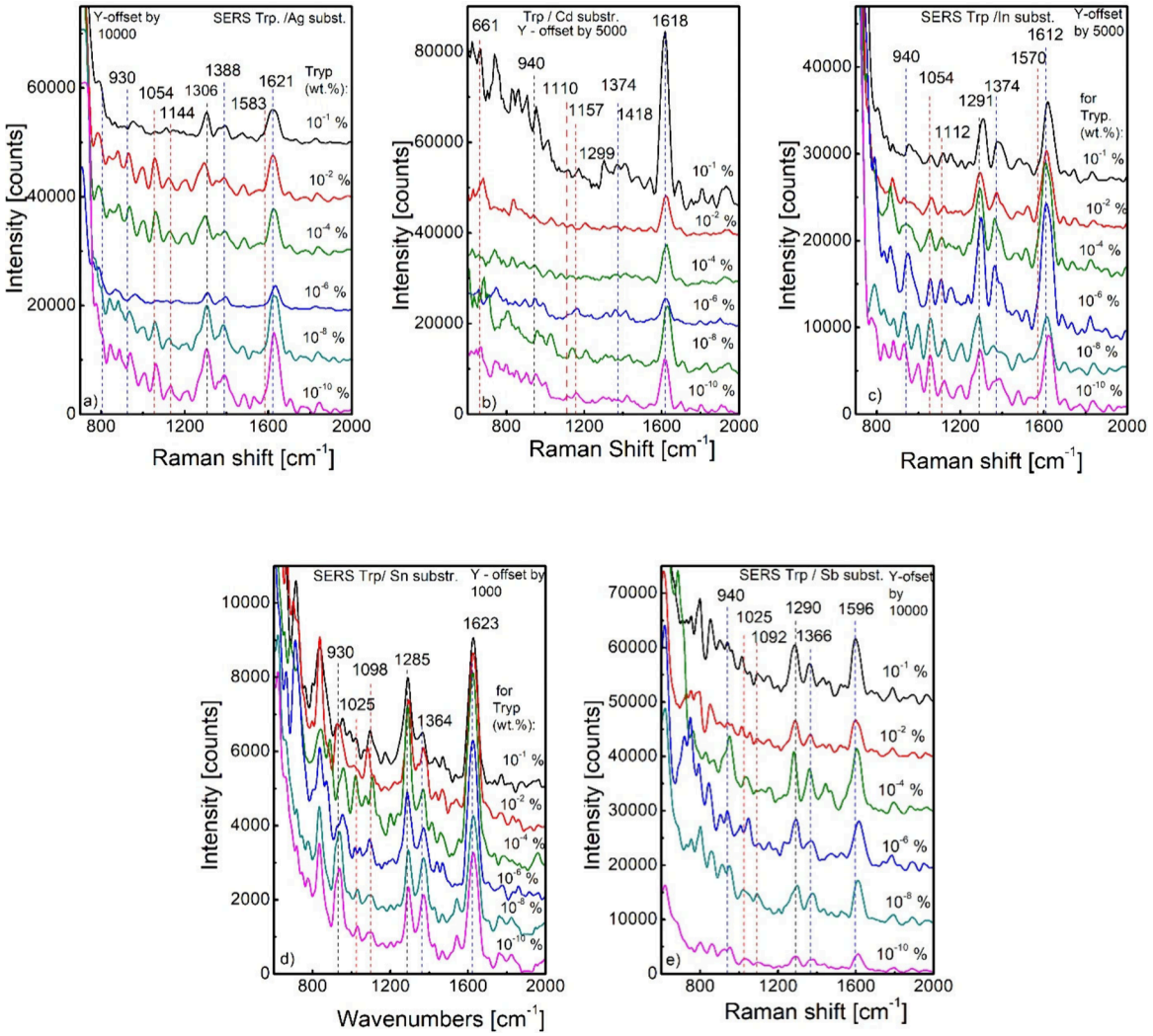

Figure 5. SERS spectra of L-tryptophan when thin films of (a) silver and different p-block metals (b) Cd, (c) In, (d) Sn, and (e) Sb are used as enhancing substrates.

nanoparticles of silver and gold in colloids are used,[11d,28b,c] as well as reports using copper,[9b] indium,[16b] and Au−Pd alloys.[28a]

As it was stated in the introduction, amino acids possess carboxylate COO^- and amino NH_3^+ groups as ligands and they act as zwitterions; i.e., depending on the pH of the surrounding medium one or both of these groups can be ionized.[2]

The common opinion is that the amino acids interact with the free electrons on the surface of nanostructures of noble metals through the amino group NH_3^+. It has been shown in the case of silver and L-tryptophan at pH = 2 that, in addition to the interaction with NH_2, an enhancement of the COO^- peaks is also observed in the SERS spectra.[28b] In the case of the remaining metals analyzed in this paper, Cd, In, Sn, and Sb, the formation of coordination compounds is discussed,[29] in which they bind simultaneously with NH_3^+ and COO^- groups.

In order to investigate the influence of the electronic structure of the material from which the nanostructures are made, we performed a series of SERS and SEF tests with aqueous solutions of L-tryptophan. Thin films with a thickness of ∼50 nm of silver, cadmium, and p-block metals (In, Sn and Sb) were used as substrates as well as thin polycrystalline coatings of the following intermetallic compounds AgCd, Ag_3In, Ag_3Sn and Ag_3Sb. The deposition methods for preparation of the intermetallic compound coatings have been described in our previous works, and more detailed information can be found in Supporting Information 1. Regarding the phase composition and the results of the X-ray diffraction of the coatings, information is given in Supporting Information 2.

Initially, we performed an analysis of the influence of the pH of L-tryptophan aqueous solutions at pH = 2 and pH = 7, in order to trace the Raman spectra when the amino group (pH 2) and carboxylate group (pH 7) were ionized. The results are given in Supporting Information 4. The solution with pH = 2 was chosen because of the increased possibility for chemical reaction between the p-block metals and L-tryptophan due to the ionized NH_3^+ amino group (Supporting Information 4, Figure S7).

Several bands are observed in all spectra. A very intense band in the frequency range 1550−1680 cm^{-1} with a maximum falling in the region 1620−1630 cm^{-1}, as well as two intense peaks at lower frequencies in the range 1200−1400 cm^{-1}, are seen; the first is located in the frequency range 1280−1310 cm^{-1}, and the maximum of the second is in the region 1360−1400 cm^{-1}. They all depend on the composition of the substrate, belong to the Raman scattering of the amino and carboxylate groups, and will be discussed in detail below. The spectra also show a series of peaks due to vibrations in the indole and pyrrole rings: 1121,

https://doi.org/10.1021/acsomega.5c01439
ACS Omega 2025, 10, 19243−19255

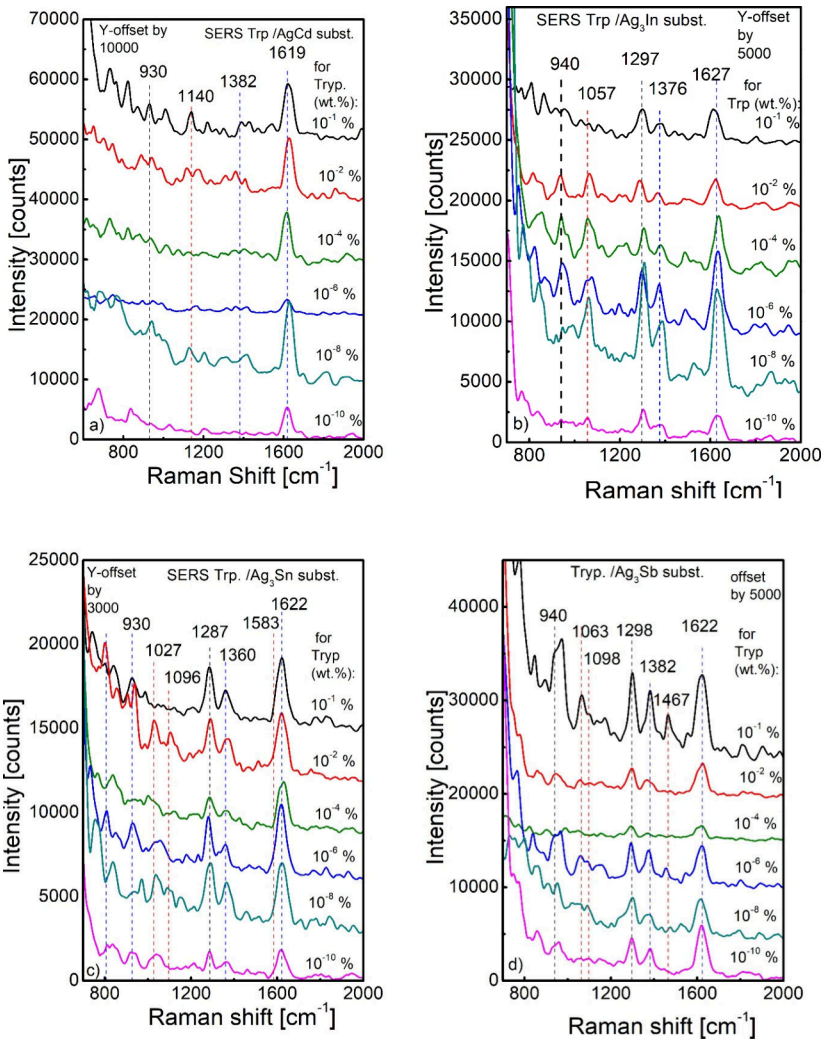

Figure 6. SERS spectra of L-tryptophan when thin films of different intermetallic compounds of silver with p-block metals used as enhancing substrates: (a) AgCd; (b) Ag_3In; (c) Ag_3Sn; (d) Ag_3Sb.

1213, 1254, and 1344 cm^{-1}, corresponding to H-scissoring of pyrrole, H-scissoring of benzene, pyrrole-stretching, H-rocking of benzene, and C−H-bending, respectively.[28b]

Below we will examine in more detail the behavior of the Raman scattering of NH_2/NH_3^+ and $COOH/COO^-$ groups in the SERS spectra of L-tryptophan using substrates of silver and p-block metals, as well as some of their intermetallic compounds.

5.1. NH_2 Group. First, we will consider the interaction of the used enhancing metallic coatings with the amino group of L-tryptophan. The SERS spectrum of L-tryptophan in an aqueous solution with pH = 2, when silver nanoparticles were used, has been extensively reviewed in ref 28b. The authors observed Raman scattering bands at 930, 1054, 1144, and 1583 cm^{-1} belonging to the vibrations of the NH_2 group. Since the peak at 1583 cm^{-1} overlaps with that of the asymmetric stretching vibrations of the COO^- group located between 1550 and 1680 cm^{-1} and is expressed as a shoulder of this peak with strong Raman scattering (Figure 5a), while the band at 930 cm^{-1} coincides with the stretching modes of the COO^- group,[28b] we will consider the vibrations of NH_2 in the frequency range of 1000−1200 cm^{-1}. When a silver layer is used as a substrate, peaks at 1054 and 1144 cm^{-1} are seen in the SERS spectra, which are due to the rocking vibration of the NH_2 group.[28b]

In the case when cadmium is used as a SERS substrate, weakly intensive peaks are observed in the region 1000−1200 cm^{-1}. Information on the influence of cadmium on the vibrational modes of the NH_2 group can be found in the case of Cd−glycine[29a] and Cd(L-Threonine) complexes.[4] The authors of ref 4 observed peaks at 1110 and 1157 cm^{-1} in the SERS spectra, which according to them can be attributed to rocking and scissoring vibration modes of the amino group. In addition, it has been theoretically and experimentally determined that the Cd−N stretching frequencies in the Cd(L-Threonine) metal-based complex are located at 668 cm^{-1} and 657 cm^{-1}. Accordingly, the weak peaks at 661 cm^{-1}, 1110 cm^{-1} and 1157 cm^{-1} in the SERS spectra of L-tryptophan can be attributed to the Cd−N stretching, rocking and scissoring vibration modes of the amino group (Figure 5b).

Peaks with significantly higher intensity are observed in the region 1000−1200 cm^{-1} when the p-block elements − In, Sn and Sb are used (Figure 5c-e). Indium preferentially forms coordination compounds with amides.[19c,21] The peaks at 1054 and 1112 cm^{-1} in the SERS spectra of L-tryptophan, obtained using thin films of indium as enhancing substrate, can be attributed to the rocking and wading vibration modes of the NH_2 group, respectively.[16b] The scissoring vibration mode of the NH_2 group is observed as a shoulder of an intense Raman

https://doi.org/10.1021/acsomega.5c01439
ACS Omega 2025, 10, 19243−19255

scattering band located between 1560 and 1670 cm^{-1}, attributed to the asymmetric stretching vibrations of the COO^- group. In the case of SERS with tin and antimony supports, peaks at 1096 and 1091 cm^{-1} are seen (Figure 5d,e), which correspond to the frequencies of the NH_2 rocking vibrations observed in the interaction of the amino group of glycine with Sn and Sb atoms in metal−organic complexes.[29d,e]

Therefore, we can assume the presence of two ways of interaction of the NH_2 group with the metals studied in this work. In the case of silver and indium, coordination compounds are formed[28b,29c,30] and the observed vibrational modes in SERS spectra in the frequency range 1000−1200 cm^{-1} of the NH_2 group in these two metals are close. In the second case, the case of Cd, Sn and Sb, metal−organic complexes are formed, according to the literature data on their interaction with other amino acids,[29a,d,e] and the frequencies of the vibrational modes depend on the coordination number of the metal ion.

In the SERS spectra of L-tryptophan when intermetallic compounds are used (Figure 6), an enhancement of the NH_2 rocking vibration peaks at 1140 cm^{-1} in the case of AgCd substrate, 1057 cm^{-1} for Ag_3In and 1098 cm^{-1} for Ag_3Sn and Ag_3Sb, is again observed. These frequencies are close to those observed in the SERS spectra of p-block metals presented in Figure 5. This suggests that the interaction mainly occurs with the p-block metal involved in the intermetallic compound.

5.2. COO^- Group. In the case of L-tryptophan on silver (Figure 5a), prominently enhanced stretching vibration modes of the COO^- group are observed at 1620, 1388 and 930 cm^{-1}, similar to the results published in ref 28b.

When using cadmium substrates (Figure 5b), a clear enhancement only of the asymmetric stretching mode of the COO^- group with a maximum at ∼1622 cm^{-1} is observed, while no significant enhancement of the symmetric mode of the COO^- group as well as the peaks due to Raman scattering from the other groups in the L-tryptophan molecule is seen. A weak peak is visible at 1374 cm^{-1} in the Raman spectra, which probably belongs to the symmetric stretching vibration of the COO^- group. The greater electronegativity of the cadmium and indium atoms, compared to that of silver,[31] suggests that they attract the carboxylate group more strongly, as a result of which an elongation of the C−O^- bond and a decrease in the vibration frequency are expected. Accordingly, the peaks at 1374 cm^{-1} in the SERS spectra of L-tryptophan on cadmium and indium substrates are due to symmetric vibrations of the C−O^- bond.

When thin films of tin and antimony are used as SERS substrates (Figure 5d,e), an additional shift is observed due to the higher atomic weight, so we can assume that the Raman scattering bands at 1364−1366 cm^{-1} are caused by interaction of these metals with the carboxylate group.

When substrates of the intermetallic compounds AgCd, Ag_3In, Ag_3Sn and Ag_3Sb are used (Figure 6), where the energy of the interband transitions from the 4d level is different, it is seen that the composition does not strongly affect the position of the peak of the asymmetric vibrations of the COO^- group. More significant changes in the SERS spectra are observed in the symmetric stretching vibration of the COO^- group located in the frequency range of 1360−1400 cm^{-1}.

Similar to the Cd substrates used, in the SERS spectra with AgCd substrates, a significant enhancement of the peak due to the asymmetric stretching vibration mode is observed. Similar to the Raman spectra of the Cd- Glutathione complex,[29b] we can assume that the peak at 1382 cm^{-1} corresponds to the symmetric stretching vibration of the COO^- group. Since the cadmium atoms have a higher electronegativity compared to that of silver, they therefore attract the COO^- group more strongly. For this reason, it can be assumed that L-tryptophan interacts with the cadmium atoms of the AgCd compound, which is the reason for the significant enhancement.

As can be seen from the band structure, in the case of Cd and Sn compounds (Figure 2) a higher photon energy is required to excite a hot hole from the d electron state of silver. In the case of SERS discussed here, an argon laser was used, whose excitation radiation photon energy of 2.54 eV (488 nm) is significantly lower, so the L-tryptophan interacts with holes formed as a result of intraband transitions of s and p electrons. In the SERS spectra of L-tryptophan, when the Ag_3In and Ag_3Sn substrates are used in the measurements (Figure 6a, b), a shift of the symmetric stretching vibration of the COO^- group to ∼1376 and 1360 cm^{-1} is observed, while in the spectrum of tryptophan on a thin Ag_3Sb film substrate (Figure 6d), the peak is again observed at a frequency of 1382 cm^{-1}. We can assume that the interaction with the COO^- group in this case is similar to that of silver. The calculated band structure of the Ag_3Sb intermetallic compound (Figure 2d) shows that the d level of silver is significantly lower than that of the silver compounds with cadmium and tin and also the electronegativity of antimony atoms is 1.9 and coincides in value with that of silver. So, we cannot expect significant differences in comparison with silver in the way of interaction of Ag_3Sb structures with amino acids.

5.3. CH_2 Group. A strong Raman scattering band is observed in the frequency range 1250−1340 cm^{-1} of the SERS spectra, which is weaker only in the case of SERS when cadmium or AgCd substrates are used. It is noteworthy that the maximum shifts from 1306 cm^{-1} in the case of silver toward the lower frequencies (1285−1297 cm^{-1}) in the case of p-block metals and the studied intermetallic compounds. According to,[29b] the peak at 1306 cm^{-1} is due to a wagging vibration mode in the CH_2 group in the case of SERS of an aqueous solution of L-tryptophan. In,[16b] a peak at 1278 cm^{-1} is observed, which the authors attribute to the CH_2 group. The theoretical calculations and experimental results in[28b] show that a bending mode is observed at 1278 cm^{-1}, which is in a plane perpendicular to the wagging vibration of the CH_2 group. So this shift can be due to a change in the enhancement of these two modes. As discussed in section 3.1, the intense bands in SERS spectra are those given by vibrations inducing polarization of the adsorbate electron cloud perpendicular to the metal surface, which suggests a certain orientation of the L-tryptophan molecule. Since the interaction of the NH_2 and COO^- groups of L-tryptophan is stronger with the p-electrons, the orientation of the p-orbitals determines the arrangement of the molecules on the metal surface.

When tracing the influence of the concentration, a decrease in the intensity enhancement of the Raman peaks is observed when the concentration of L-tryptophan in the aqueous solution decreases from 10^{-1} wt % to 10^{-4}−10^{-6} wt %, depending on the enhancing material used. At concentrations lower than 10^{-6} wt %, an increase in the intensity is observed. We can assume that in the concentration range of 10^{-1} − 10^{-4} wt % the number of molecules in the solution is large and several layers of L-tryptophan molecules are formed on the metal grains. Under concentrations of 10^{-4} − 10^{-6} wt % L-tryptophan, it can be assumed that the number of analyzed molecules is already small enough, so that the coverage of the metal grains can be considered as a single layer. A comparison of the enhancement at the same concentration of 10^{-8} wt %. is shown in Figure 7.

https://doi.org/10.1021/acsomega.5c01439
ACS Omega 2025, 10, 19243−19255

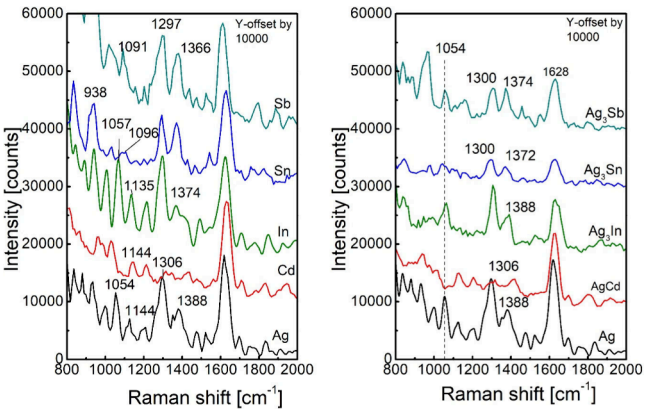

Figure 7. Comparison of SERS spectra of L-tryptophan water solutions at a concentration of 10^{-8} wt % on different enhancing substrates.

6. SEF OF L-TRYPTOPHAN

The study of typtophan fluorescence wavelength is an important tool in bioanalysis, which provides information about changes in the structure of organic compounds.[12b] We conducted a series of tests on the emission of L-tryptophan using a 254 nm line of a Hg lamp for excitation. The photon energy of 4.88 eV is chosen to be greater than the energy of interband transitions (see Figures 2 and 3). The author of ref 2 states that the fluorescence emission of L-tryptophan appears in the range of 310−420 nm, as its maximum depends on the pH of the solution: 347 nm for acidic media; 353 nm for neutral, and 360 nm for basic solutions. The emission spectra measured by us are presented in Figure 8. It can be seen that when solutions with pH = 2 were used (Figure 8a), a low intensity of the emission band is observed even at the highest concentration used in the present work (0.1 wt % L-tryptophan in H_2O), which is probably due to the quenching effect observed in solutions of tryptophan at low pH.[2,32]

Enhancement of the L-tryptophan emission is observed in the case of pH = 7. Figure 8b and c shows the emission spectra in the case of a concentration of 10^{-2} wt % L-tryptophan in H_2O. It can be seen in Figure 8b that the least enhancement is observed in the case of silver, while the measured emission intensity using thin films of Cd and Sn is almost 2 times greater, and the fluorescence emission signal measured using a clean glass substrate is below the sensitivity of the instrument used. It can be assumed that the interband transitions from the d level play a role in the lower fluorescence intensity of L-tryptophan in the case of a silver substrate, while in the case of the other metals only the valence s and p electrons are involved. Significant enhancement of the fluorescence signal was observed when substrates of intermetallic compounds AgCd and Ag_3In were used (Figure 8c). At this concentration of tryptophan (10^{-2} wt %) in the aqueous solution, the maximum of the emission line is at 353 nm. This wavelength coincides with the position of the maximum observed in the case of an aqueous solution of tryptophan in a pH neutral medium; i.e., both the amino and the carboxylate groups are ionized. Therefore, although enhancement is observed, we can assume that we still have a contribution from noninteracting L-tryptophan molecules in the entire volume of the solution. We can assume that two mechanisms play a role in the enhancement. In the case of intermetallic compounds, the d level of silver is located significantly deeper below the Fermi level compared to pure silver. Hot holes are formed during interband transitions, which have higher energy and therefore higher mobility and therefore lose their energy faster due to electron−hole and phonon interactions.

Another factor that can contribute to the enhancement of the emission is the participation of LSPR. It has been shown that AgCd and Ag_3In nanostructures[24f,a] have a maximum LSPR excitation efficiency in the spectral region 3.5−5 eV, while Ag_3Sn and Ag_3Sb have a maximum LSPR excitation at photon energies less than 3.5 eV.[25c,d]

A decrease in the intensity of the emission band with decreasing the concentration was observed, as in the case of 10^{-4} wt % L-tryptophan in H_2O (Figure 8d, e) a very weak fluorescence signal was registered when Ag substrate was used (Figure 8d). The greatest enhancement is seen when a AgCd substrate is used. A shift of the maximum position toward the longer wavelengths occurs in all spectra, which is typical for the fluorescence emission of L-tryptophan upon interaction with metals. In the case of AgCd and Ag_3In substrates, signal enhancement was observed even at concentrations lower than 10^{-4} wt % L-tryptophan in H_2O, and it is noticeable that the red shift of the maximum position continues.

7. CONCLUSIONS AND FUTURE OUTLOOK

The possibility of using p-block metals and their intermetallic compounds in surface-enhanced spectroscopic techniques is considered in this work. The interaction between the substrate and the analyte is of great importance for these techniques. The usage of intermetallic alloys allows variation of the interband transition energy, as in this way the catalytic activity of the nanostructures is determined and the places of molecular absorption are defined. These studies are still in their early stages, focusing mainly on Ag−Au, Au−Pd, and Au−Cu alloys and nanoparticles. Since silver is highly reactive to the environment, the addition of a p-block element can significantly improve the chemical stability of the plasmonic nanostructures.

The alloys and intermetallic compounds of silver and p-block metals allow variation of the interband transition energy and their engineering in a very wide spectral region. By choosing a p-block element and its concentration in the bimetallic alloys, the energy of interband transitions can be further tuned in a relatively larger energy range covering the short-wavelength part of the visible spectral region and the ultraviolet region up to 4 eV.

This range can be extended by using alloys and intermetallic p-block compounds with other noble metals such as gold, platinum and copper. Since the interband transitions in gold are observed at smaller photon energy in comparison with those of silver, their alloys are suitable for tuning the excitation frequency of gold nanostructures in the visible spectral region.

The interaction between the substrate and the analyzed object can be controlled by tuning the energy of interband transitions and, respectively, the energies of photoexcited electrons and holes as well as the photon energy of the exciting laser irradiation. By this way, an amplification for certain bands in SERS can be achieved. This effect is also used in a number of other molecular diagnostic techniques to indicate the ratio of the intensities of certain bands.

The role of interband transitions in the case of the interaction of amino and carboxylate groups of tryptophan with the SERS substrate is discussed in the present work, but it can be applicable for all amino acids and various compounds containing other functional groups, such as Anthranilic acid (containing NH_2 and OH^- groups), Psilocybin (with NH and PO_4^- functional groups).

https://doi.org/10.1021/acsomega.5c01439
ACS Omega 2025, 10, 19243−19255

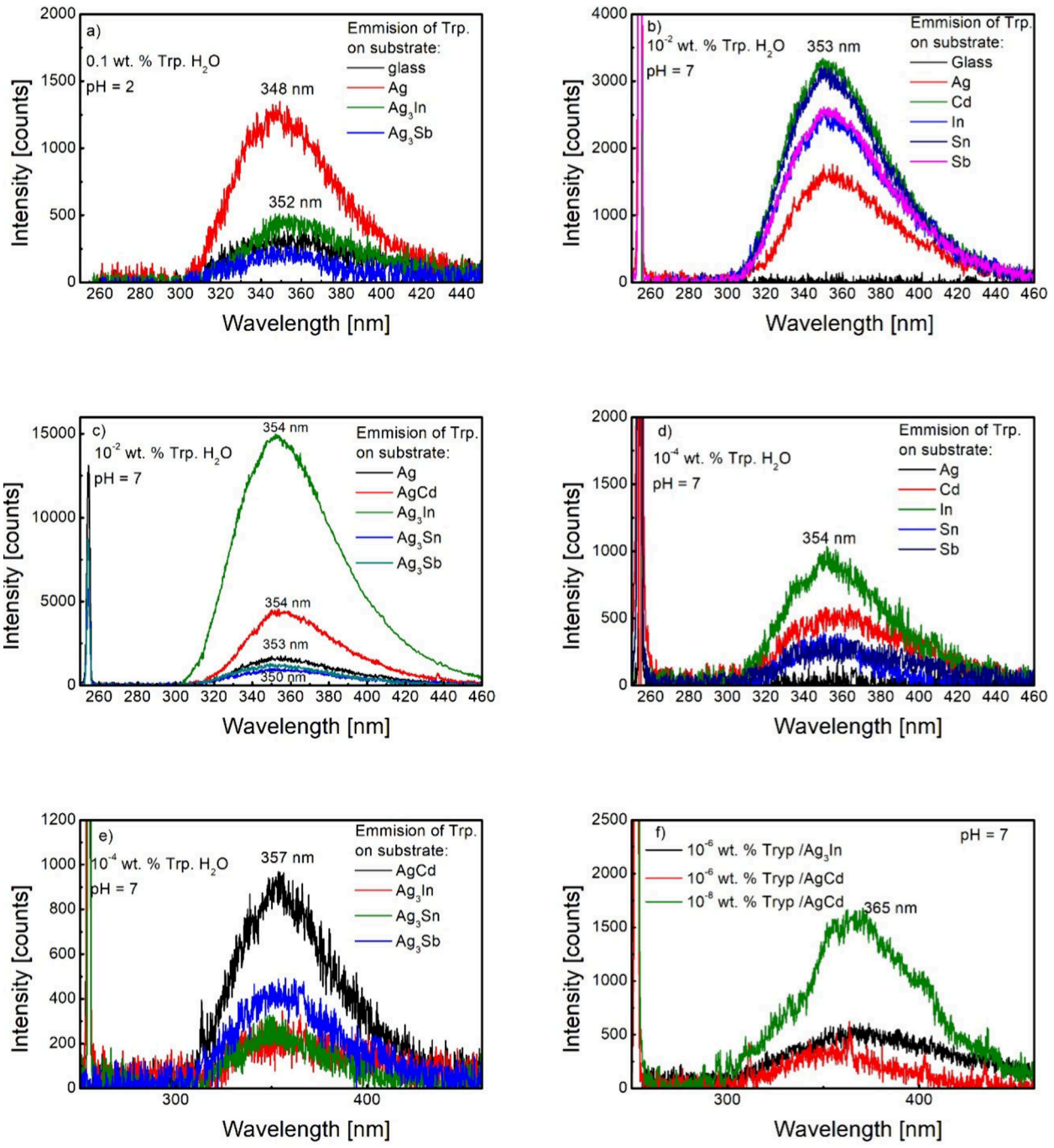

Figure 8. Emission spectra of tryptophan (Trp.) with different concentrations in H_2O when different p-block metals substrates are used: (a) 0.1 wt % Trp. (pH = 2); (b) 10^{-2} wt % Trp. (pH = 7); (d) 10^{-4} wt % Trp. (pH = 7). Emission of tryptophan when intermetallic compounds of silver and p-block metals are used: (c) 10^{-2} wt % Trp. (pH = 7); (e) 10^{-4} wt % Trp. (pH = 7); (f) emission spectra of Trp. at concentrations 10^{-6} and 10^{-8} wt % on Ag_3In and AgCd substrates.

A good understanding and control of the interaction between the SERS substrate and a specific functional group will allow in some cases the use of substrates without a previously applied capture agent for specific biodiagnostic purposes.

The realization of selective capture of certain groups will allow us not only to find applications in Surface enhanced spectroscopies for diagnostics but also to control the choice of capturing agents on the SERS substrate. By this way, a better selectivity of the SERS substrate will be achieved.

A simple setup is used in the experiments presented in this paper, which shows possibilities for modeling and production of a cheaper equipment with application in biodiagnostics, which will be significantly smaller, even with portable dimensions, and thus suitable for smaller medical laboratories. By having an appropriate database for the investigated biological objects, the medical staff could be able to perform initial analysis quickly at the place, even without having profound knowledge of SERS technology.

Besides the perspectives of p-block elements for diagnostics without interaction with the human body presented here, despite their common toxicity, they could also be used for active medical purposes, as carrier agents for interventions that use

https://doi.org/10.1021/acsomega.5c01439
ACS Omega 2025, 10, 19243−19255

optical sources, drug delivery, etc., due to their inertization through chelation with the biological molecules. This perspective requires further investigations involving specialists in medicine and biology and the development of methods and strategies for preparing chemically stable nanosized objects from p-block metals and their compounds that can be safely introduced into humans.

■ ASSOCIATED CONTENT

Supporting Information

The Supporting Information is available free of charge at https://pubs.acs.org/doi/10.1021/acsomega.5c01439.

Additional information about the preparation of the L-tryptophan solutions, the deposition of the enhancing layers together with their morphological and structural peculiarities, the DFT calculations, and the SERS and SEF measurements (PDF)

■ AUTHOR INFORMATION

Corresponding Author

Rosen Todorov − *Institute of Optical Materials and Technologies "Acad. J. Malinowski", Bulgarian Academy of Sciences, 1113 Sofia, Bulgaria;* orcid.org/0000-0002-7674-1476; Email: rossen@iomt.bas.bg

Author

Temenuga Hristova-Vasileva − *Institute of Optical Materials and Technologies "Acad. J. Malinowski", Bulgarian Academy of Sciences, 1113 Sofia, Bulgaria; Institute of Solid State Physics, Bulgarian Academy of Sciences, 1784 Sofia, Bulgaria;* orcid.org/0000-0002-0929-5277

Complete contact information is available at: https://pubs.acs.org/10.1021/acsomega.5c01439

Notes

The authors declare no competing financial interest.

Biographies

Dr. Rosen Todorov got a PhD in Physics in 2001 from the Institute of Optical Materials and Technology of the Bulgarian Academy of Sciences and has been an Associate Professor at the same institute since 2010. His research interests are in the field of deposition of thin semiconductor and metal coatings and multilayer structures, and characterization of their optical properties. Since 2019, he has been directing his research in the field of searching and development of new materials for UV plasmonics. In his research, he investigates the role of intermetallic compounds and alloys of silver and gold as plasmonic materials and the possibility of tuning their spectral region of plasmonic activity.

Dr. eng. Temenuga Hristova-Vasileva got a PhD in Materials Science from the University of Chemical Technology and Metallurgy (Sofia, Bulgaria) and was habilitated in Condensed Matter Physics at the Institute of Solid State Physics of the Bulgarian Academy of Sciences. She is proficient in materials synthesis, and physical and physicochemical characterization of inorganic materials. Since 2018 she works in the field of development and investigation of intermetallic alloys and compounds for plasmonics. Her main research interests are pointed towards development of new approaches for physical deposition, as well as preparation and engineering of new materials.

■ ACKNOWLEDGMENTS

The authors gratefully acknowledge the 23rd International School on Condensed Matter Physics, Varna, Bulgaria and ACS Omega for the invitation and opportunity to present their scientific findings.

■ REFERENCES

(1) Alberts, B.; Johnson, A.; Lewis, J.; Raff, M.; Roberts, K.; Walter, P. *Molecular biology of the cell*, 4th ed.; Garland Science: New York, 2002.

(2) Konev, S. V. *Fluorescence and phosphorescence of proteins and nucleic acids*; Springer Science & Business Media, 2012.

(3) Liu, L.; Jia, L.; Yang, W.; Xiao, Y.; Dai, J.; Cui, P.; Zhou, L.; Yin, Q. Measurement and correlation of L-tryptophan in aqueous solutions with a wide range of pH and different monovalent counterions from 283.15 to 323.15 K. *J. Solution Chem.* **2023**, *52*, 228−250.

(4) (a) Várnagy, K.; Sóvágó, I.; Kozłowski, H. Transition metal complexes of amino acids and derivatives containing disulphide bridges. *Inorg. Chim. Acta* **1988**, *151* (2), 117−123. (b) Chetry, N.; Gomti Devi, Th.; Karlo, T. Synthesis and characterization of metal complex amino acid using spectroscopic methods and theoretical calculation. *J. Mol. Struct.* **2022**, *1250*, 131670. (c) Ghatak, S. K.; Dey, D.; Sen, S.; Sen, K. Aromatic amino acids in high selectivity bismuth(iii) recognition. *Analyst.* **2013**, *138*, 2308−2314. (d) Czylkowska, A.; Szczesio, M.; Pietrzak, A.; Raducka, A.; Rogalewicz, B. Novel coordination polymer of cadmium (II) with L-tryptophan. *Materials.* **2020**, *13* (10), 2266. (e) Kawamura, K.; Igarashi, Sh.; Yotsuyanagi, T. Acceleration effect of L-tryptophan on metal ion exchange reaction of cadmium(II) with watersoluble-porphyrin-lead(II) complex and its application to stopped-flow spectrophotometric determination of nM Level of cadmium(II). *Anal. Sci.* **1988**, *4*, 175−179.

(5) (a) Severin, K.; Bergs, R.; Beck, W. Bioorganometallic chemistry - transition metal complexes with α-amino acids and peptides. *Angew. Chem.* **1998**, *37* (12), 1634−1654. (b) Beck, W. Metal Complexes of biologically important ligands, CLXXII [1]. Metal ions and metal complexes as protective groups of amino acids and peptides − reactions at coordinated amino acids. *Z. Naturforsch. B* **2009**, *64* (11−12), 1221−1245.

(6) (a) Aaseth, J.; Crisponi, G.; Andersen, O. *Chelation Therapy in the Treatment of Metal Intoxication*; Academic press, Elsevier, 2016. (b) Part 1: Bioremediation of inorganic pollutants. In *"Handbook of Bioremediation: Physiological, Molecular and Biotechnological Interventions*; Hasanuzzaman, M.; Prasad, M. N. V., Eds.; Academic press, Elsevier, 2021. (c) Selden, C. R.; Schilling, K.; Godfrey, L.; Yee, N. Metal-binding amino acid ligands commonly found in metalloproteins differentially fractionate copper isotopes. *Sci. Rep.* **2024**, *14* (1), 1902. (d) Sonker, N.; Verma, S.; Kumar, C.; Ansari, K. M.; Verma, S. K. Do heavy metals have a role in extrahepatic portal vein obstruction in children: A pilot case-control study. *Clin. Epidemiol. Global Health.* **2024**, *28*, 101628. (e) Alzahrani, O. M.; Abo-Amer, A. E.; Mohamed, R. M. Improvement of Zn (II) and Cd (II) biosorption by Priestia megaterium PRJNA526404 isolated from agricultural waste water. *Microorganisms.* **2022**, *10* (12), 2510. (f) Remelli, M.; Nurchi, V. M.; Lachowicz, J. I.; Medici, S.; Zoroddu, M. A.; Peana, M. Competition between Cd (II) and other divalent transition metal ions during complex formation with amino acids, peptides, and chelating agents. *Coord. Chem. Rev.* **2016**, *327*, 55−69.

(7) (a) *Surface Analysis and Techniques in Biology*; Smentkowski, V. S., Ed., Springer: Cham, 2014. (b) Kasemo, B. Biological surface science. *Surf. Sci.* **2002**, *500* (1−3), 656−677. (c) Stahelin, R. V. Surface plasmon resonance: a useful technique for cell biologists to characterize biomolecular interactions. *Mol. Biol. Cell* **2013**, *24* (7), 883−1093. (d) de Oliveira Neto, J. G.; Viana, J. R.; Butarelli, A. L.; dos Santos, A. P.; Lage, M. R.; dos Santos, A. O. Synthesis, physicochemical properties, and antitumor cytotoxic activity of the Mg (II) coordination complex containing 1, 10-phenanthroline and sulfate ligands. *Inorg. Chim. Acta* **2023**, *556*, 121658. (e) Lien, M. C.; Yeh, I. H.; Tadepalli, S.; Liu, K. K. ZnO Nanocages decorated with Au@ AgAu yolk−shell

nanomaterials for SERS-based detection of hyperuricemia. *ACS Omega.* **2024**, *9* (14), 16160−16167.
(8) (a) *SERS for point-of-care and clinical applications*; Fales, A., Ed.; Elsevier, 2022. (b) Fischer, W. B.; Eysel, H. H. Polarized Raman spectra and intensities of aromatic amino acids phenylalanine, tyrosine and tryptophan. *Spectrochim. Acta, Part A* **1992**, *48* (5), 725−732.
(9) (a) Liz-Marzán, L. M.; Willets, K. A.; Chen, X. Fifty years of surface-enhanced spectroscopy. *ACS Nano* **2024**, *18* (8), 5995−5997. (b) Święch, D.; Palumbo, G.; Piergies, N.; Kollbek, K.; Marzec, M.; Szkudlarek, A.; Paluszkiewicz, C. Surface modification of Cu nanoparticles coated commercial titanium in the presence of tryptophan: Comprehensive electrochemical and spectroscopic investigations. *Appl. Surf. Sci.* **2023**, *608*, 155138. (c) Pięta, E.; Paluszkiewicz, C.; Kwiatek, W. M. Multianalytical approach for surface-and tip-enhanced infrared spectroscopy study of a molecule−metal conjugate: Deducing its adsorption geometry. *Phys. Chem. Chem. Phys.* **2018**, *20* (44), 27992−28000.
(10) (a) Choi, N.; Schlücker, S. Convergence of surface-enhanced Raman scattering with molecular diagnostics: a perspective on future directions. *ACS Nano* **2024**, *18* (8), 5998−6007. (b) Tran, V. A.; Tran, T. T. V.; Le, V. T.; Doan, V. D.; Vo, G. N.L.; Tran, V. H.; Jeong, H.; Vo, T. T. T. Advanced nano engineering of surface-enhanced Raman scattering technologies for sensing applications. *Appl. Mater. Today.* **2024**, *38*, 102217. (c) Sen, T.; Haldar, K. K.; Patra, A. Au nanoparticle-based surface energy transfer probe for conformational changes of BSA protein. *J. Phys. Chem. C* **2008**, *112* (46), 17945−17951. (d) Mostufa, S.; Rezaei, B.; Ciannella, S.; Yari, P.; Gómez-Pastora, J.; He, R.; Wu, K. Advancements and perspectives in optical biosensors. *ACS Omega.* **2024**, *9* (23), 24181−24202.
(11) (a) Baia, M.; Astilean, S.; Iliescu, T. *Raman and SERS investigations of pharmaceuticals*; Springer Science & Business Media, 2008. (b) Pérez-Jiménez, A. I.; Lyu, D.; Lu, Z.; Liu, G.; Ren, B. Surface-enhanced Raman spectroscopy: benefits, trade-offs and future developments. *Chem. Sci.* **2020**, *11* (18), 4563−4577. (c) Quezada, C.; Samhitha, S.; Salas, A.; Ges, A.; Barraza, L. F.; Palacio, D. A.; Esquivel, S.; Blanco-López, M. C.; Sánchez-Sanhueza, G.; Meléndrez, M. F. Surface-enhanced Raman sensor with molecularly imprinted nanoparticles as highly sensitive recognition material for cancer marker amino acids. *Talanta.* **2024**, *278*, 126465. (d) Valera, P. S.; Henriques-Pereira, M.; Wagner, M.; Gaspar, V. M.; Mano, J. F.; Liz-Marzán, L. M. Surface-enhanced Raman scattering monitoring of tryptophan dynamics in 3D pancreatic tumor models. *ACS Sensors.* **2024**, *9* (8), 4236−4247. (e) Rippa, M.; Castagna, R.; Brandi, S.; Fusco, G.; Monini, M.; Chen, D.; Zhou, J.; Zyss, J.; Petti, L. Octupolar plasmonic nanosensor based on ordered arrays of triangular Au nanopillars for selective rotavirus detection. *ACS Appl. Nano Mater.* **2020**, *3* (5), 4837−4844. (f) Li, W.; Zhang, Y.; Zhang, W.; Hu, P.; Zhang, M.; Meng, X.; Zhang, X.; Shang, M.; Duan, X.; Wang, C. Portable SERS-based POCT kit for ultrafast and sensitive determining paraquat in human gastric juice and urine. *ACS Omega.* **2024**, *9* (16), 18576−18583. (h) Murugappan, S.; Tofail, S. A.; Thorat, N. D. Raman spectroscopy: a tool for molecular fingerprinting of brain cancer. *ACS Omega.* **2023**, *8* (31), 27845−27861.
(12) (a) Eisinger, J.; Navon, G. Fluorescence quenching and isotope effect of tryptophan. *J. Chem. Phys.* **1969**, *50* (5), 2069−2077. (b) Vivian, J. T.; Callis, P. R. Mechanisms of tryptophan fluorescence shifts in proteins. *Biophys. J.* **2001**, *80* (5), 2093−2109. (c) Liu, H.; Zhang, H.; Jin, B. Fluorescence of tryptophan in aqueous solution. *Spectrochim. Acta, Part A* **2013**, *106*, 54−59. (d) Singla, N.; Bhadram, V. S.; Narayana, C.; Chowdhury, P. White light generation by carbonyl based indole derivatives due to proton transfer: an efficient fluorescence sensor. *J. Phys. Chem. A* **2013**, *117* (13), 2738−2752. (e) Han, M.; Feng, J.; Wang, X.; Wang, J.; Liu, Y.; Zhao, R.; Mu, Y. Synthesis and biological evaluation of esculetin derivatives as antidiabetic agents. *J. Mol. Struct.* **2025**, *1324*, 140942.
(13) (a) Guo, Z.; Yu, G.; Zhang, Z.; Han, Y.; Guan, G.; Yang, W.; Han, M. Y. Intrinsic optical properties and emerging applications of gold nanostructures. *Adv. Mater.* **2023**, *35* (23), 2206700. (b) Dahan, K. A.; Li, Y.; Xu, J.; Kan, C. Recent progress of gold nanostructures and their applications. *Phys. Chem. Chem. Phys.* **2023**, *25* (28), 18545−18576.
(14) (a) Blaber, M. G.; Arnold, M. D.; Ford, M. J. A review of the optical properties of alloys and intermetallics for plasmonics. *J. Phys.: Condens. Matter.* **2010**, *22* (14), 143201. (b) Gong, C.; Leite, M. S. Noble metal alloys for plasmonics. *ACS Photonics.* **2016**, *3* (4), 507−513. (c) Todorov, R.; Hristova-Vasileva, T.; Katrova, V.; Atanasova, A. Silver and gold containing compounds of p-block elements as perspective materials for UV plasmonics. *ACS Omega.* **2023**, *8* (16), 14321−14341. (d) Ross, M. B.; Schatz, G. C. Aluminum and indium plasmonic nanoantennas in the ultraviolet. *J. Phys. Chem. C* **2014**, *118* (23), 12506−12514. (e) Collette, R.; Wu, Y.; Olafsson, A.; Camden, J. P.; Rack, P. D. Combinatorial thin film sputtering Au_xAl_{1-x} alloys: correlating composition and structure with optical properties. *ACS Comb. Sci.* **2018**, *20* (11), 633−642. (f) Kelly, K. L.; Coronado, E.; Zhao, L. L.; Schatz, G. C. The optical properties of metal nanoparticles: the influence of size, shape, and dielectric environment. *J. Phys. Chem. B* **2003**, *107* (3), 668−677.
(15) Pilot, R.; Signorini, R.; Durante, C.; Orian, L.; Bhamidipati, M.; Fabris, L. A review on surface-enhanced Raman scattering. *Biosensors.* **2019**, *9* (2), 57.
(16) (a) Gray, S. K. Theory and modeling of plasmonic structures. *J. Phys. Chem. C* **2013**, *117* (5), 1983−1994. (b) Das, R.; Soni, R. K. Synthesis and surface-enhanced Raman scattering of indium nanotriangles and nanowires. *RSC Adv.* **2017**, *7* (51), 32255−32263. (c) Rippa, M.; Castagna, R.; Tkachenko, V.; Zhou, J.; Petti, L. Engineered nanopatterned substrates for high-sensitive localized surface plasmon resonance: An assay on biomacromolecules. *J. Mater. Chem. B* **2017**, *5* (27), 5473−5478.
(17) (a) Long, L.; Ju, W.; Yang, H. Y.; Li, Z. Dimensional design for surface-enhanced Raman spectroscopy. *ACS Mater. Au.* **2022**, *2* (5), 552−575. (b) Chen, Y.; Fan, Z.; Zhang, Z.; Niu, W.; Li, C.; Yang, N.; Chen, B.; Zhang, H. Two-dimensional metal nanomaterials: synthesis, properties, and applications. *Chem. Rev.* **2018**, *118* (13), 6409−6455. (c) Shao, M.; Ji, C.; Tan, J.; Du, B.; Zhao, X.; Yu, J.; Man, B.; Xu, K.; Zhang, C.; Li, Z. Ferroelectrically modulate the Fermi level of graphene oxide to enhance SERS response. *Opto-Electron. Adv.* **2023**, *6* (11), 230094−1. (d) Liu, Y.; Qiao, S.; Fang, C.; He, Y.; Sun, H.; Liu, J.; Ma, Y. A highly sensitive LITES sensor based on a multi-pass cell with dense spot pattern and a novel quartz tuning fork with low frequency. *Opto-Electron. Adv.* **2024**, *7* (3), 230230. (e) Wu, Y.; Sun, T.; Shao, M.; Ji, C.; Li, C.; Zhang, C.; Li, Z. Pyroelectrically driven charge transfer and its advantages on SERS and self-cleaning property. *Laser Photonics Rev.* **2025**, *19* (4), 2401152.
(18) (a) Moskovits, M. Surface roughness and the enhanced intensity of Raman scattering by molecules adsorbed on metals. *J. Chem. Phys.* **1978**, *69* (9), 4159−4161. (b) Moskovits, M. Surface-enhanced spectroscopy. *Rev. Mod. Phys.* **1985**, *57* (3), 783−826.
(19) (a) Eftink, M. R.; Ghiron, C. A. Fluorescence quenching studies with proteins. *Anal. Biochem.* **1981**, *114* (2), 199−227. (b) Polemi, A.; Shuford, K. L. Distance dependent quenching effect in nanoparticle dimers. *J. Chem. Phys.* **2012**, *136*, 184703. (c) Sukharev, M.; Freifeld, N.; Nitzan, A. Numerical Calculations of Radiative and Non-Radiative Relaxation of Molecules Near Metal Particles. *J. Phys. Chem. C* **2014**, *118* (20), 10545−10551. (d) Ghosh, D.; Chattopadhyay, N. Gold and silver nanoparticles based superquenching of fluorescence: A review. *J. Lumin.* **2015**, *160*, 223−232.
(20) (a) Xu, H.; Hepel, M. "Molecular beacon"-based fluorescent assay for selective detection of glutathione and cysteine. *Anal. Chem.* **2011**, *83* (3), 813−819. (b) Zhang, Z.; Liu, N.; Zhang, Z.; Xu, D.; Ma, S.; Wang, X.; Zhou, T.; Zhang, G.; Wang, F. Construction of aptamer-based molecular beacons with varied blocked structures and targeted detection of thrombin. *Langmuir.* **2021**, *37* (29), 8738−8745.
(21) (a) Peña-Rodríguez, O. Modelling the dielectric function of Au-Ag alloys. *J. Alloys Compd.* **2017**, *694*, 857−863. (b) Ha Pham, T. T.; Vu, X. H.; Dien, N. D.; Trang, T. T.; Van Truong, N.; Thanh, T. D.; Tan, P. M.; Ca, N. X. The structural transition of bimetallic Ag−Au from core/shell to alloy and SERS application. *RSC Adv.* **2020**, *10* (41), 24577−24594. (c) Sultangaziyev, A.; Ilyas, A.; Dyussupova, A.;

https://doi.org/10.1021/acsomega.5c01439
ACS Omega 2025, 10, 19243−19255

Bukasov, R. Trends in application of SERS substrates beyond Ag and Au, and their role in bioanalysis. *Biosensors.* **2022**, *12* (11), 967. (d) Sun, Y.; Zhang, Y.; Ren, H.; Qiu, H.; Zhang, S.; Lu, Q.; Hu, Y. Highly sensitive SERS sensors for glucose detection based on enzyme@ MOFs and ratiometric Raman. *Talanta.* **2024**, *271*, 125647.

(22) (a) Lyu, P.; Espinoza, R.; Nguyen, S. C. Photocatalysis of metallic nanoparticles: interband vs intraband induced mechanisms. *J. Phys. Chem. C* **2023**, *127* (32), 15685−15698. (b) Sun, M.; Wang, A.; Zhang, M.; Zou, S.; Wang, H. Interband and intraband hot carrier-driven photocatalysis on plasmonic bimetallic nanoparticles: A case study of Au−Cu alloy nanoparticles. *ACS Nanosci. Au.* **2024**, *4* (5), 360−373. (c) Lee, D.; Yoon, S. Plasmonic switching: hole transfer opens an electron-transfer channel in plasmon-driven reactions. *J. Phys. Chem. C* **2020**, *124* (29), 15879−15885.

(23) Zhao, J.; Li, L.; Li, P.; Dai, L.; Dong, J.; Zhou, L.; Wang, Y.; Zhang, P.; Ji, K.; Zhang, Y.; Yu, H.; et al. Realization of 2D metals at the ångström thickness limit. *Nature.* **2025**, *639*, 354−359.

(24) (a) McMahon, J. M.; Gray, S. K.; Schatz, G. C. Ultraviolet plasmonics: The poor metals Al, Ga, In, Sn, Tl, Pb, and Bi. *Phys. Chem. Chem. Phys.* **2013**, *15*, 5415−5423. (b) Green, E. L.; Muldawer, L. Optical properties of the alphaphase alloys Ag-Zn and Ag-Cd. *Phys. Rev. B* **1970**, *2*, 330−340. (c) Nicholson, J. A.; Riley, J. D.; Leckey, R. C. G.; Jenkin, J. G.; Liesegang, J.; Azoulay, J. Ultraviolet photoelectron spectroscopy of the valence bands of some Au alloys. *Phys. Rev. B* **1978**, *18* (6), 2561. (d) Riley, J. D.; Leckey, R. C. G.; Jenkin, J. G.; Liesegang, J.; Poole, R. T. Ultraviolet photoelectron spectra of the outer d bands of Ag-In and Ag-Cd alloys. *J. Phys. F.* **1976**, *6* (2), 293. (e) Keast, V. J.; Barnett, R. L.; Cortie, M. B. First principles calculations of the optical and plasmonic response of Au alloys and intermetallic compounds. *J. Phys.: Condens. Matter.* **2014**, *26*, 305501. (f) Todorov, R.; Hristova-Vasileva, T.; Katrova, V.; Atanasova, A.; Milushev, G. Electronic structure and plasmonic activity in co-evaporated Ag-In bimetallic alloys. *J. Alloys Compd.* **2022**, *897*, 163253.

(25) (a) Todorov, R.; Hristova-Vasileva, T.; Katrova, V.; Strijkova, V.; Atanasova, A.; Milushev, G. Formation, structure, and optical performance of $AgCd/Ag_5Cd_8$ phases in thin film form. *J. Mater. Sci.: Mater. Electron.* **2023**, *34* (13), 1093. (b) Wronkowska, A. A.; Wronkowski, A.; Kuklinski, K.; Senski, M.; Skowronski, L. Spectroscopic ellipsometry study of the dielectric response of Au-In and Ag-Sn thin-film couples. *Appl. Surf. Sci.* **2010**, *256*, 4839−4844. (c) Katrova, V.; Hristova-Vasileva, T.; Atanasova, A.; Strijkova, V.; Todorov, R. Optical properties of nanostructured bimetallic films from the Ag-In and Ag-Sb systems and their surface enhanced fluorescence application. *J. Phys.: Conf. Ser.* **2022**, *2240*, No. 012007. (d) Atanasova, A.; Katrova, V.; Hristova-Vasileva, T.; Todorov, R. Synthesis, microstructure, and optical properties of Ag_3Sn nanoparticles for plasmonic sensing applications. *Proc. SPIE* **2021**, *11919*, 1191927.

(26) Ashcroft, N. W.; Mermin, N. D. *Solid State Physics*; Saunders, 1976.

(27) (a) Rasul, H. H.; Mamad, D. M.; Azeez, Y. H.; Omer, R. A.; Omer, K. A. Theoretical investigation on corrosion inhibition efficiency of some amino acid compounds. *Comput. Theor. Chem.* **2023**, *1225*, 114177. (b) Hssain, A. H.; Devi, T. G.; Salih, R. O.; Abdullah, N. R. Structural and spectroscopic study of L-tryptophan dimer state using DFT and MD: computational and experimental analysis. *J. Mol. Struct.* **2025**, *1331*, 141582.

(28) (a) Gerami, M.; Farrokhpour, H.; Orangi, N. Charge transfer surface-enhanced Raman and absorption spectra of the zwitterionic form of cysteine adsorbed on M@ Au12 (M= Au, Ag, Pt, and Pd) nanoclusters. *J. Phys. Chem. A* **2023**, *127* (18), 3991−4004. (b) Chuang, C. H.; Chen, Y. T. Raman scattering of L-tryptophan enhanced by surface plasmon of silver nanoparticles: vibrational assignment and structural determination. *J. Raman Spectrosc.* **2009**, *40* (2), 150−156. (c) Zhang, Q.; Guan, Q.; Han, S.; Yan, X.; Hong, J.; Duan, L.; Wu, G.; Hong, Y.; Yu, L.; Wang, C. Highly sensitive SERS detection of tryptophan based on diazo coupling reaction using two derivatization reagents. *Microchem. J.* **2024**, *207*, 112241.

(29) (a) Krishnan, K.; Plane, R. A. Raman study of glycine complexes of zinc (II), cadmium (II), and beryllium (II) and the formation of mixed complexes in aqueous solution. *Inorg. Chem.* **1967**, *6* (1), 55−60. (b) Glušič, M.; Ropret, P.; Vogel-Mikuš, K.; Grdadolnik, J. The binding sites of cadmium to a reduced form of glutathione. *Acta Chim. Slov.* **2013**, *60* (1), 61−69. (c) Avila-Montiel, C.; Tlahuext, H.; Ariza, A.; Godoy-Alcántar, C.; Tapia-Benavides, A. R.; Tlahuextl, D. M. Indium coordination compounds derived from amino amides. *Eur. J. Inorg. Chem.* **2022**, *2022* (20), No. e202200178. (d) Novikova, G. V.; Petrov, A. I.; Staloverova, N. A.; Samoilo, A. S.; Dergachev, I. D.; Shubin, A. A. Complex formation of Sn (II) with glycine: An IR, DTA/TGA and DFT investigation. *Spectrochim. Acta, Part A* **2015**, *135*, 491−497. (e) Voit, E. I.; Udovenko, A. A.; Kovaleva, E. V.; Makarenko, N. V.; Beleneva, I. A.; Zemnukhova, L. A. Structure and properties of the molecular complex of antimony (III) fluoride with γ-glycine. *J. Struct. Chem.* **2019**, *60* (4), 630−639.

(30) Yadav, J. S.; Antony, A.; George, J.; Subba Reddy, B. V. Recent developments in indium metal and its salts in organic synthesis. *Eur. J. Org. Chem.* **2010**, *2010* (4), 591−605.

(31) Pauling, L. *The Nature of the Chemical Bond*, 3rd ed.; Cornell University Press, 1960; p 93.

(32) Pan, C. P.; Muiño, P. L.; Barkley, M. D.; Callis, P. R. Correlation of tryptophan fluorescence spectral shifts and lifetimes arising directly from heterogeneous environment. *J. Phys. Chem. B* **2011**, *115* (12), 3245−3253.

https://doi.org/10.1021/acsomega.5c01439
ACS Omega 2025, 10, 19243−19255